



Nuclear-Order-Induced Quantum Criticality and Heavy-Fermion Superconductivity at Ultra-low Temperatures in YbRh₂Si₂

Erwin Schuberth¹, Steffen Wirth² and Frank Steglich^{2,3*}

¹Physics Department, Technical University of Munich, Munich, Germany, ²Max Planck Institute for Chemical Physics of Solids, Dresden, Germany, ³Center for Correlated Matter, Zhejiang University, Hangzhou, China

The tetragonal heavy-fermion metal YbRh₂Si₂ orders antiferromagnetically at $T_N = 70$ mK and exhibits an unconventional quantum critical point (QCP) of Kondo-destroying type at $B_N = 60$ mT, for the magnetic field applied within the basal (a , b) plane. Ultra-low-temperature magnetization and heat-capacity measurements at very low fields indicate that the 4f-electronic antiferromagnetic (AF) order is strongly suppressed by a nuclear-dominated hybrid order (“A-phase”) at $T_A \leq 2.3$ mK, such that quantum critical fluctuations develop at $B \approx 0$ (Schuberth et al., Science, 2016, 351, 485–488). This enables the onset of heavy-fermion superconductivity ($T_c = 2$ mK) which appears to be suppressed by the primary antiferromagnetic order at elevated temperatures. Measurements of the Meissner effect reveal bulk superconductivity, with T_c decreasing under applied field to $T_c < 1$ mK at $B > 20$ mT. The observation of a weak but distinct superconducting shielding signal at a temperature as high as 10 mK suggests the formation of insulated random islands with emergent A-phase order and superconductivity. Upon cooling, the shielding signal increases almost linearly in temperature, indicating a growth of the islands which eventually percolate at $T \approx 6.5$ mK. Recent electrical-resistivity results by Nguyen et al. (Nat. Commun., 2021, 12, 4341) confirm the existence of superconductivity in YbRh₂Si₂ at ultra-low temperatures. The combination of the results of Schuberth et al. (2016) and Nguyen et al. (2021) at ultra-low temperatures below B_N , along with those previously established at higher temperatures in the paramagnetic state, provide compelling evidence that the Kondo-destruction quantum criticality robustly drives unconventional superconductivity.

Keywords: heavy fermion, superconductivity, quantum criticality, Kondo destruction, nuclear order

1 KONDO-DESTROYING, FIELD-INDUCED QUANTUM CRITICAL POINT

Lanthanide-based intermetallic compounds showing heavy-fermion phenomena are well understood within the framework of the Kondo lattice (Wirth and Steglich, 2016). The localized open 4f-shells of such materials are characterized by a distinct hierarchy of fundamental energy scales, the local Coulomb repulsion and Hund’s rule energies, spin-orbit coupling, crystal-field splitting, Kondo screening including excited crystal-field states at an elevated temperature, where the

OPEN ACCESS

Edited by:

Jeffrey W. Lynn,
National Institute of Standards and
Technology (NIST), United States

Reviewed by:

Hyunsoo Kim,
Missouri University of Science and
Technology, United States
Huixia Luo,
Sun Yat-Sen University, China

*Correspondence:

Frank Steglich
steglich@cps.mpg.de

Specialty section:

This article was submitted to
Superconducting Materials,
a section of the journal
Frontiers in Electronic Materials

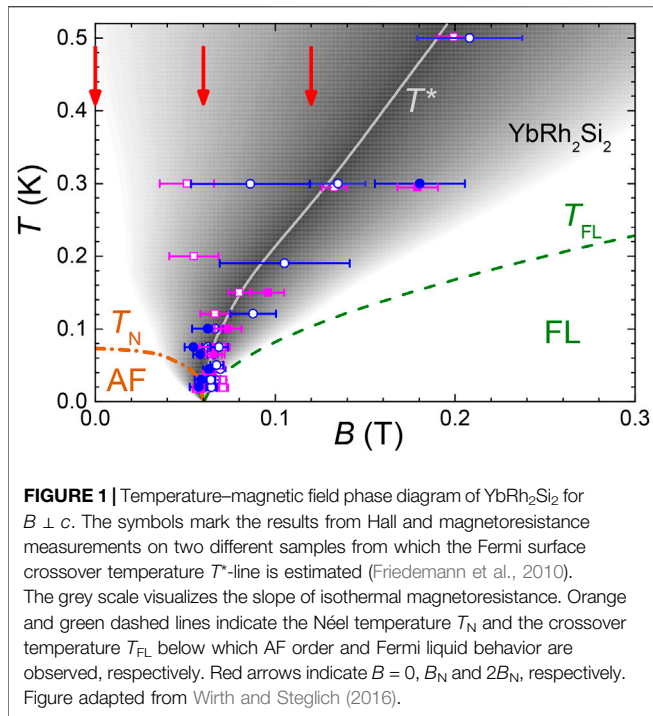
Received: 04 February 2022

Accepted: 01 March 2022

Published: 17 May 2022

Citation:

Schuberth E, Wirth S and Steglich F
(2022) Nuclear-Order-Induced
Quantum Criticality and Heavy-
Fermion Superconductivity at Ultra-low
Temperatures in YbRh₂Si₂.
Front. Electron. Mater. 2:869495.
doi: 10.3389/femat.2022.869495



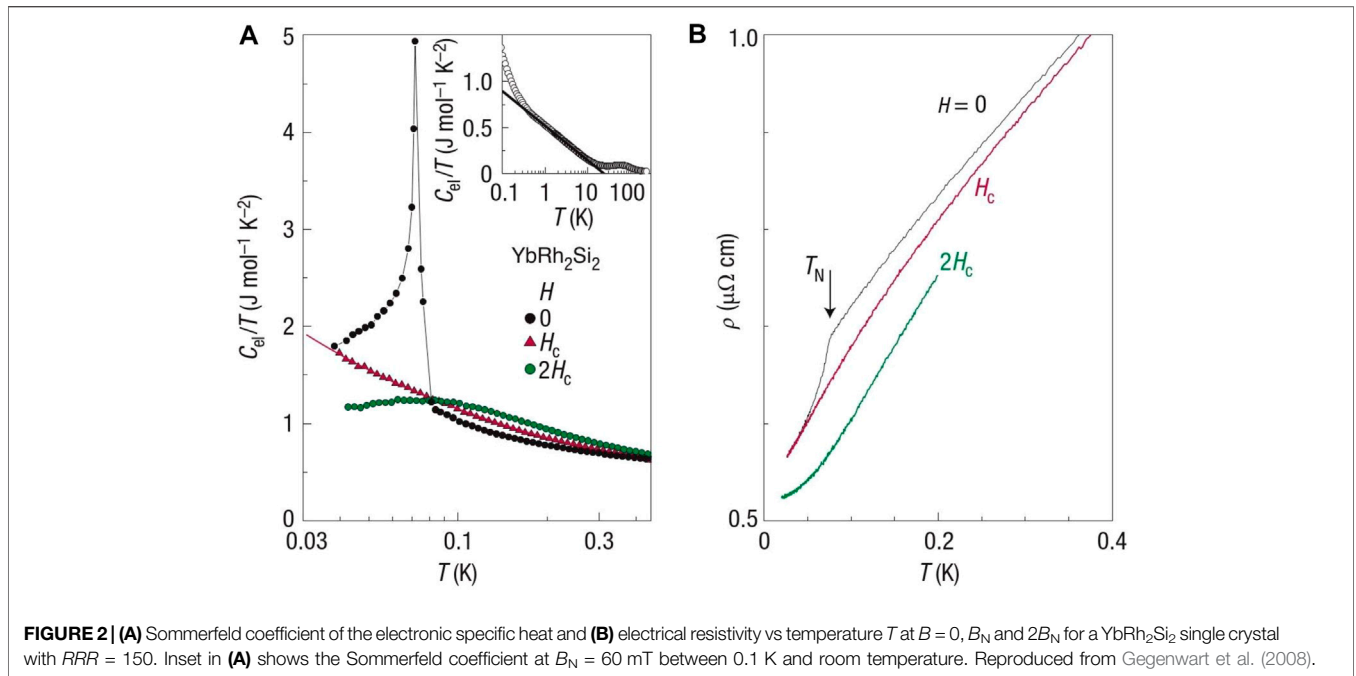
formation of hybridized $4f$ -bands starts to be recognized in ARPES measurements (Chen et al., 2017), as well as Kondo screening of the lowest-lying crystal-field-derived Kramers doublet ($k_B T_K$). As illustrated below, the single-ion Kondo temperature T_K was found to be identical to T_{coh} (Ernst et al., 2011; Seiro et al., 2018) where spatial coherence among $4f$ -shells sets in as seen in transport measurements.

The onsite Kondo screening competes with the inter-site magnetic Ruderman-Kittel-Kasuya-Yosida (RKKY) interaction. While predominant Kondo screening results in a paramagnetic heavy-fermion ground state, a dominant RKKY interaction causes magnetic, most frequently antiferromagnetic (AF), order. For a substantial number of these heavy-fermion metals the Kondo screening turns out to almost exactly cancel the RKKY interaction. In this situation, a continuous transition may exist at $T = 0$ between the heavy-fermion and the AF phase. This continuous quantum phase transition or quantum critical point (QCP) can be tuned by a non-thermal control parameter, e.g., pressure or magnetic field (Stewart, 2001; von Löhneysen et al., 2007; Gegenwart et al., 2008; Sachdev, 2011).

YbRh₂Si₂ is a prototypical heavy-fermion metal (Köhler et al., 2008; Ernst et al., 2011) which orders antiferromagnetically at a Néel temperature $T_N = 70$ mK (Trovarelli et al., 2000). Because of a strong magnetic anisotropy the critical field B_N at which AF order smoothly disappears is only 60 mT when the field is applied within the basal tetragonal (a , b) plane, i.e., it is more than ten times lower compared to $B_N \parallel c$ (Gegenwart et al., 2002). The staggered moment was shown to be very small, $\mu_{AF} \approx 0.002 \mu_B$ (Ishida et al., 2003). Both the low-temperature paramagnetic ($B > B_N$) and AF phases ($B < B_N$) behave as heavy Fermi liquids (Gegenwart et al., 2002) whereas a funnel-shaped quantum

critical regime in the B - T phase diagram (Figure 1) with non-Fermi-liquid properties is centered at the critical field B_N . The AF phase transition is of second order to the lowest temperature (20 mK) accessible in magnetostriction measurements (Gegenwart et al., 2007); the crossover between the paramagnetic Fermi liquid and the non-Fermi-liquid phase turns out to be quite broad. The sub-linear white $T^*(B)$ crossover line in Figure 1 was constructed by the midpoints of thermally broadened jumps in both the longitudinal magnetoresistivity and the isothermally measured initial normal Hall coefficient (Paschen et al., 2004; Friedemann et al., 2010). They agree satisfactorily with the locations of distinct anomalies in the field dependence of both the isothermal DC magnetization and magnetostriction as well as in the temperature dependence of the AC susceptibility measured at fixed magnetic field (Gegenwart et al., 2007). $T^*(B)$ indicates a crossover between a small Fermi volume (“small Fermi surface”) at low fields and a large one at elevated fields. The crossover width (grey shaded region) turns out to be proportional to T . The QCP at $B_N(T = 0)$ is of an unconventional “local” (instead of itinerant) variety, which may be called a “partial Mott” or Kondo-destroying QCP. It is characterized by a dynamical spin susceptibility with frequency-over-temperature scaling and a fractional exponent in the singular parts of both the frequency and temperature dependences (Coleman et al., 2001; Si et al., 2001) as observed by inelastic neutron scattering on both UCu_{5-x}Pd_x (Aronson et al., 1995) and CeCu_{6-x}Au_x (Schröder et al., 2000). The latter material (von Löhneysen et al., 1994) as well as CeRhIn₅ (Shishido et al., 2005; Park et al., 2006) are also prototypical heavy-fermion metals exhibiting a local QCP.

Figure 2 displays the thermal evolution at low temperatures of both the (Sommerfeld) coefficient of the $4f$ -derived part of the specific heat, $\gamma = C_{el}/T = C_{4f}/T$ (Figure 2A), and the electrical resistivity measured on an YbRh₂Si₂ single crystal with a low residual resistivity of about $0.5 \mu\Omega$ cm (Figure 2B), at $B = 0$, B_N and $2B_N$, respectively (see red arrows in Figure 1). The behavior of a heavy Fermi liquid in both the AF and low-temperature paramagnetic phase is clearly resolved by a huge constant γ -value (Figure 2A) and a pronounced T^2 -dependence in $\rho(T)$ (Figure 2B). Very peculiarly, the Fermi liquid in the AF phase (with small Fermi surface as $T \rightarrow 0$) is considerably heavier than the Fermi liquid in the paramagnetic phase (with large Fermi surface). Approaching the QCP at $B = B_N$ by cooling below 0.3 K, one finds that $\gamma(T)$ diverges following a power-law dependence with a critical exponent of ≈ -0.3 (Custers et al., 2003). As shown in the inset of Figure 2A, $\gamma(T)$ obeys a logarithmic T -dependence (Custers et al., 2003) at elevated temperature. The incremental resistivity measured at $B = B_N$ on a very clean single crystal is strictly linear in T , $\Delta\rho(T) = \rho(T) - \rho_0 = A'T$, at $T < 0.1$ K. Over a broad temperature range up to $T = 10$ K, the resistivity semi-quantitatively follows a T -linear dependence, although the “temperature-dependent resistivity exponent”, defined as $d \ln(\rho - \rho_0)/d \ln T$, shows some variation that is clustered around 1 (Westerkamp, 2009). For a single crystal with nominally 5% Ge substituted for Si showing a five times larger residual resistivity, $\Delta\rho(T) = A'T$ is more strictly observed all the way up to $T = 10$ K (Custers et al., 2003), which



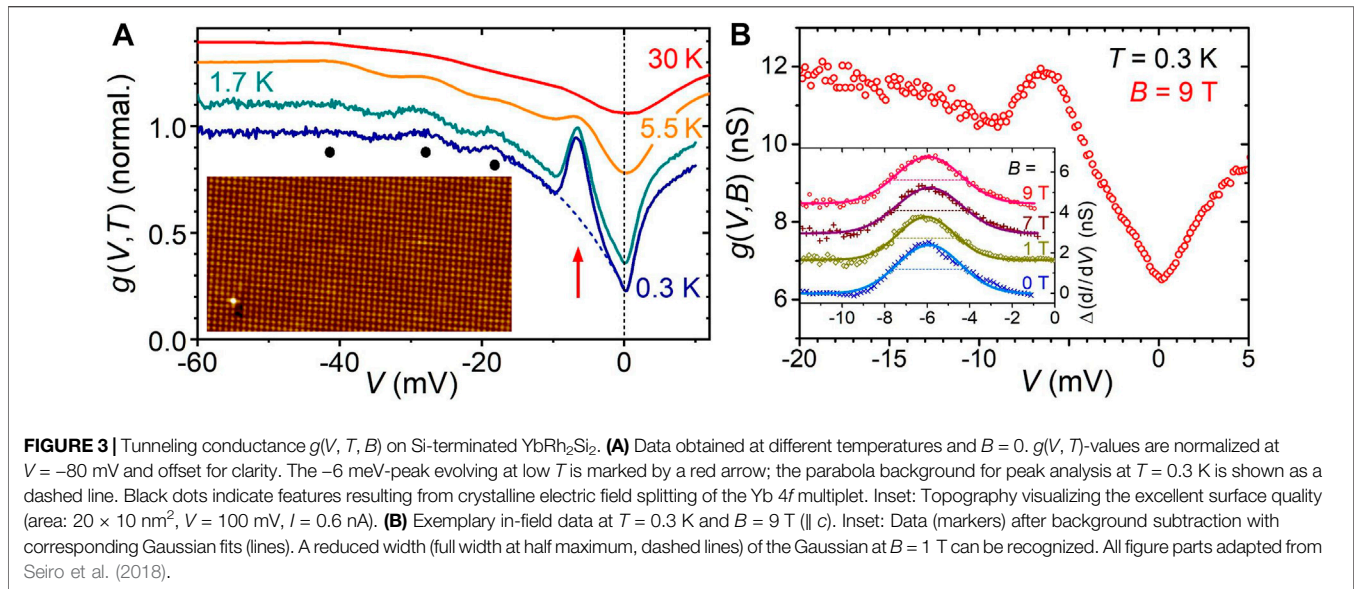
suggests a degree of disorder modulation to this “strange-metal” behavior. If one restricts to a relatively narrow temperature range, $\Delta\rho(T)$ has also been fit with other exponents, $A''T^\alpha$ ($\alpha < 1$); this includes the case of $\alpha = 3/4$ in the temperature window $0.4 \text{ K} < T < 1 \text{ K}$ for the high-quality crystal exploited in **Figure 2B**, as motivated by the theory of “critical quasiparticles” (Wölfle and Abrahams, 2011) (which, however, is inapt to explain the measured asymptotic linear-in- T dependence of the resistivity at the unconventional QCP in YbRh₂Si₂). Most importantly, though, for all samples studied so far, the asymptotic ($T \rightarrow 0$) T -dependence of $\rho(T)$ registered at $B = B_N$ is found to be linear, see also Nguyen et al. (2021). The linear-in- T coefficient, A' , can be converted to a linear-in- T coefficient in the scattering rate, $1/\tau$, in a procedure based on a Drude analysis: the latter is found to be much smaller than what appears in a Planckian form when a “background” heavy-fermion value is used for the effective mass (Nguyen et al., 2021; Taupin and Paschen, 2022).

One of the important techniques that provides new insight into such correlation-driven phenomena is scanning tunneling spectroscopy (STS) with its unique ability to give local, atomically resolved information that relates to the one-particle Green’s function (Kirchner et al., 2020). However, one of the prerequisites for successful STS measurements is the preparation and perpetuation of clean sample surfaces. Fortunately, YbRh₂Si₂ can be cleaved nicely perpendicular to the c -axis in ultra-high vacuum (UHV) and at low temperatures of about 20 K providing atomically flat surface areas of often several hundreds of nanometers in extent. Such surfaces not only evidence the excellent sample quality (inset to **Figure 3A**), they even allow to analyze the defects to be mostly caused by Rh-atoms on Si sites (Wirth et al., 2012).

We here focus on predominantly encountered Si-terminated surfaces. In case of such surfaces, the Kondo-active Yb atoms are

located in the fourth-to-topmost layer which prevents a reduced screening of the Yb local moments at the surface (Alexandrov et al., 2015) and ensures a predominant study of bulk properties by STS. The latter is clearly evidenced by the observation of crystal field excitations in the tunneling spectra (Ernst et al., 2011) at energies in excellent agreement with inelastic neutron scattering data (Stockert et al., 2006b) (black dots in **Figure 3A**). Moreover, Si-terminated surfaces promote predominant tunneling into the conduction band as compared to the $4f$ quasiparticle states and thereby simplify the analysis of the obtained spectra as co-tunneling can be neglected (Ernst et al., 2011; Kirchner et al., 2020). In this simplified picture, the successive formation of the single-ion Kondo effect upon lowering the temperature results primarily in a modification of the density of states of the conduction band seen as a strong decrease of the tunneling conductance $g(V, T)$ for V small enough to not break up the quasiparticles. This process is observed to commence at around 100 K and coincides with the onset of local Kondo screening involving excited crystalline electric field levels as concluded from entropy estimates (Custers et al., 2003). Upon cooling to below the single-ion Kondo temperature $T_K \simeq 25 \text{ K}$ the $4f$ electrons condense into the Kramers doublet ground state and the Kondo lattice develops. This is reflected in the STS data, **Figure 3A**, by the strong development of a peak at around -6 meV . Notably, the position in energy of this peak does not depend on temperature.

The relation of this -6 meV -peak to the Kondo lattice is supported by calculations: Results of a multi-level finite- U non-crossing approximation (Ernst et al., 2011) which does not consider intersite Kondo correlations captures the temperature evolution of the zero-bias conductance dip remarkably well but provides no indication for a peak at -6 meV . Conversely, renormalized band structure calculations



(Zwicknagl, 2011) which treats the fully renormalized Kondo lattice ground state finds a partially developed hybridization gap at slightly smaller energy in the quasiparticle density of states (which is complementary to the here measured density of states of the conduction band within the Kondo regime).

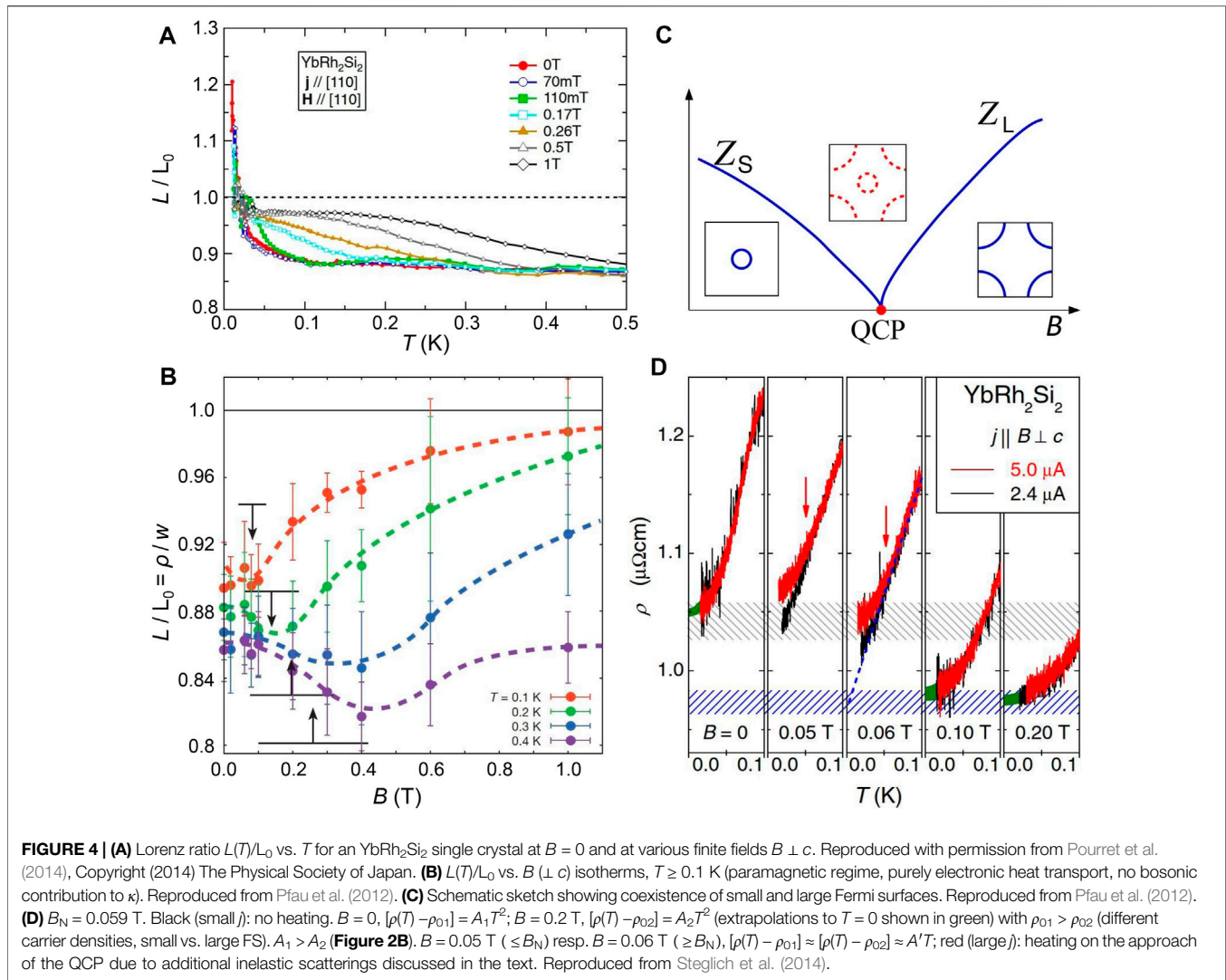
Albeit this Kondo lattice peak sets in at around T_K , i.e., $T_{\text{coh}} \approx T_K$ as mentioned above, it only slowly increases in height down to about 3 K $\approx 0.1 T_{\text{coh}}$, cf. tunneling conductance at 5.5 K in **Figure 3A**. This, along with a further decrease of $g(T)$ around zero bias, may explain why single-ion descriptions can often be applied to temperatures well below T_K despite neglected lattice Kondo effects (Coleman et al., 1985; Sun and Steglich, 2013). Only below about 3 K, the -6 meV-peak gains considerably in height indicating dominant lattice Kondo correlations at these low temperatures. This is in line with magneto- (Friedemann et al., 2010) and thermal transport (Hartmann et al., 2010) investigations. In particular, the comparison of the STS data with thermopower measurements indicates the formation of a medium-heavy Fermi liquid down to about 3 K while strong non-Fermi liquid behavior sets in only below this temperature. Apparently, quantum criticality only sets in if there is sufficient buildup of lattice Kondo correlations at low enough temperatures (Seiro et al., 2018). A similar conclusion is suggested by resonant angle-resolved photoemission spectroscopy on CeRhIn₅ (Chen et al., 2018).

STS was also conducted at 0.3 K for magnetic fields applied $B \parallel c$, see exemplary data for $B = 9$ T in **Figure 3B**. It should be noted that renormalized band structure calculations (Zwicknagl, 2011) predict a smooth quasiparticle disintegration up to well above 30 T in YbRh₂Si₂ while AF order is already suppressed at $B \approx 0.6$ T for $B \parallel c$. The position in energy of the Kondo lattice signature peak at -6 meV is not influenced by applying a magnetic field, further supporting its attribution. After background subtraction it can be well fitted by a Gaussian, cf. inset of **Figure 3B**. The width of the Gaussian fit is somewhat reduced at $B = 1$ T compared to peak widths at zero field and at

several Tesla. Here we note that a field magnitude of 1 T is close to the T^* -line (cf. **Figure 1**) for $T = 0.3$ K and $B \parallel c$. Therefore, the reduced peak width at $B = 1$ T is consistent with a reduced quasiparticle weight related to quantum criticality, see also **Figure 4C**. However, these STS data on their own do not allow to distinguish between different scenarios for quantum criticality and should be extended to lower temperatures.

Consequently, the question concerning the nature of the “local” QCP in YbRh₂Si₂ and the associated critical excitations remains. To answer this question, combined thermal and electrical transport investigations on YbRh₂Si₂ single crystals were carried out down to 25 mK at zero field, close to B_N and up to $B = 1$ T ($\gg B_N$) (Pfau et al., 2012). Subsequently, Pourret et al. (2014) were able to extend such measurements down to even 8 mK. The main quantity to study in this context is the Lorenz number $L = \rho\kappa/T$, where ρ is the electrical resistivity and κ the thermal conductivity. By defining the thermal resistivity as $w = L_0 T/\kappa$, with $L_0 = (\pi k_B)^2/3e^2$ being Sommerfeld’s constant, the Lorenz ratio $L(T)/L_0$ can be written as $L/L_0 = \rho/w$. If the Wiedemann-Franz law is valid ($L(T \rightarrow 0)/L_0 = 1$), which strictly holds for elastic scattering only, the residual electrical and thermal resistivities turn out to be identical: $\rho_0/w_0 = 1$.

Very different phenomena can cause a violation of this law: 1) Fermionic excitations like spinons, i.e., charge-neutral heat carriers, may lead to $L(T \rightarrow 0)/L_0 > 1$. This was indeed concluded from measurements on, e.g., LiCuVO₄ (Parfen’eva et al., 2004). 2) Alternatively, an enhanced $w(T)$ can lead to $L/L_0 < 1$, as frequently observed at finite temperature with dominating inelastic scatterings of the charge carriers, like the ones from acoustic phonons. In the zero-temperature limit, however, inelastic scatterings have to disappear. To our knowledge, before 2012 this latter kind of violation of the Wiedemann-Franz law, $L(T \rightarrow 0)/L_0 < 1$, has never been convincingly established. For example, for the quasi-two-dimensional (2D) heavy-fermion metal CeCoIn₅, where an AF QCP was suspected



(Singh et al., 2007; Zaum et al., 2011) but not identified, $L(T)/L_0$ was extrapolated to about 0.8 as $T \rightarrow 0$ for c -axis transport at $B \approx B_{c2} \approx 5$ T, while it approaches $L(T)/L_0 \approx 1$ for in-plane ($\perp c$) transport (Tanatar et al., 2007). This result was ascribed to the action of anisotropic spin fluctuations, although as $T \rightarrow 0$, spin fluctuations as bosonic excitations must disappear as well. Subsequently, the observations by Tanatar et al. could be consistently explained within the framework of quasi-2D transport (Smith and McKenzie, 2008).

In the following, we describe the violation of the Wiedemann-Franz law in YbRh₂Si₂ with the aid of Figure 4, see also (Smidman et al., 2018). As shown in Figure 4A at $B = 0$ and 0.07 T, $L(T)/L_0 \approx 0.87$ in an extended temperature window (0.1 K $< T < 0.5$ K) (Pourret et al., 2014). In this T -range, the underlying electrical and thermal resistivities depend linearly on T , so that the electronic Lorenz ratio L_{el}/L_0 is temperature-independent. While for $\rho(T)$ the “strange-metal” behavior persists to the lowest accessible temperature, and most likely to absolute zero, an additional bosonic contribution $\kappa_m(T)$ (by magnons at $B = 0$, resp.

paramagnons at $B = 0.07$ T) is added to the electronic thermal conductivity $\kappa_{el}(T)$ at $T \leq 0.1$ K which means that here, the total thermal resistivity $\omega(T) = [\kappa_{el}(T) + \kappa_m(T)]^{-1}$ drops, and a distinct upturn develops in $L(T)/L_0$, as clearly seen in Figure 4A. Because of its bosonic nature, this additional term has to vanish as $T \rightarrow 0$, whereby it must pass over a maximum below the low- T limit of the experiments (8 mK). The (constant) low- T value of $L_{el}/L_0 \approx 0.87$, displayed in Figure 4A over an extended temperature window, is also derived from the minimum value of the $L(B)/L_0$ isotherm for $T = 0.1$ K, the lowest temperature at which no interfering paramagnon contribution to $\kappa(T)$ exists (red data points in Figure 4B). These data were obtained with a different set up on a different single crystal. We thus conclude that the ratio $\rho_0/w_0 = \rho_0/w_{el,0}$ is reduced by about 10% compared with unity, the value expected from the Wiedemann-Franz law. Figure 4B demonstrates that below 1 K, the Lorenz ratio is generally less than unity which implies predominating inelastic scattering processes, i.e., the ordinary small-angle electron-electron and electron-spin fluctuation

scatterings. As already mentioned, in this low-temperature range, a broad minimum shows up in the $L(B)/L_0$ isotherms displayed in the figure, which points to an *additional inelastic scattering process*. This minimum is found to occur around the $T^*(B)$ -line and to become narrower upon cooling. We therefore consider it to represent the dynamical origin of local quantum criticality in YbRh₂Si₂ by ascribing it to scatterings that are associated with the transformation between a small and a large Fermi surface, which coexist on either side of $T^*(B)$ all the way down to the QCP ($T = 0, B = B_N$). As displayed in **Figure 4C**, the quasiparticle weights on both sides are smoothly vanishing as $T \rightarrow 0$, whereby the minimum in $L(B)/L_0$ becomes a delta function, resulting from *fermionic* quantum critical fluctuations (which is a rare case, as in most scenarios quantum critical fluctuations are of *bosonic* origin). Apparently, these critical fluctuations are instrumental to enhance the residual thermal resistivity by about 10% over its electrical counterpart.

Several groups have reported very similar experimental data compared with those by Pfau et al. (2012), but questioned the interpretation sketched above. The key problem is the correct treatment of the bosonic term $\kappa_m(T)$. This term was just ignored by Machida et al. (2013); Reid et al. (2014), i.e., here the measured thermal conductivity was erroneously regarded as the electronic contribution in the whole low-temperature range of the experiments, down to 40 mK. On the other hand, Taupin et al. (2015), who gave a detailed interpretation of the data previously published by Pourret et al. (2014), consider $\kappa_m(T)$ to set in at a temperature as low as 30 mK, although the data (Pourret et al., 2014) clearly prove this to occur already at about 0.1 K (**Figure 4A**). Therefore, on extrapolating the data to $T = 0$ from just above 30 mK where $\kappa_m(T)$ dominates, they miss the intrinsic value $L_{el}(T \rightarrow 0)/L_0 \approx 0.9$ and instead obtain accidentally ≈ 0.97 . This leads to their false claim that the Wiedemann-Franz law holds in YbRh₂Si₂. A violation of the Wiedemann-Franz law was subsequently also reported for another heavy-fermion metal, YbAgGe (Dong et al., 2013).

In **Figure 4D**, the conclusions drawn from the heat-conduction study discussed above are nicely confirmed by results of measurements of the electrical resistivity (Lausberg, 2013). Close to the critical field $B_N = 59$ mT and at sufficiently low temperatures, the sample under investigation becomes heated by a moderate current due to its deteriorated heat conductivity. No heating is observed when applying a low enough current. Away from B_N , in the AF phase at $B = 0$ as well as in the paramagnetic phase at 0.1 and 0.2 T, the resistivity follows the Fermi liquid-type T^2 -dependence, independent of the size of the here investigated currents. Upon approaching B_N from either side, at the lowest accessible temperatures “strange-metal” behavior, characteristic of the local QCP, is observed at low current. If these linear T -dependences of $\rho(T)$ obtained at $2.4 \mu\text{A}$ are extrapolated to $T = 0$, $\rho(T)$ ends up at very different values of the residual resistivity. In particular, the so extrapolated ρ_0 values match nicely with those obtained by extrapolating the Fermi liquid-type T^2 -dependences of $\rho(T)$ found at $B = 0$ and way above B_N , respectively. We consider this jump in ρ_0 as a direct visualization of the abrupt change in the

charge-carrier density of YbRh₂Si₂ on field tuning through the Kondo-destroying QCP.

2 COMPETITION BETWEEN NUCLEAR AND PRIMARY 4f-ELECTRONIC ORDER, EMERGENCE OF HYBRID A-PHASE AND SUPERCONDUCTIVITY

When YbRh₂Si₂ single crystals were investigated by resistivity measurements at $T > 10$ mK, and specific-heat as well as susceptibility measurements at $T > 18$ mK, no superconductivity could be detected (Custers et al., 2003). The most natural explanation for this is that superconductivity becomes suppressed by the AF order which forms at $T_N = 70$ mK. To find out whether superconductivity in YbRh₂Si₂ shows up at $T \leq 10$ mK, magnetization, susceptibility and specific-heat measurements have been carried out down to temperatures as low as 0.8 mK by using a nuclear demagnetization cryostat providing a base temperature of $400 \mu\text{K}$ (Schuberth et al., 2016). Here, a total of five different single crystals was investigated. In **Figure 5A**, the temperature dependence of the field-cooled (fc) DC-magnetization, measured at a magnetic field of 0.09 mT, reveals two phase-transition anomalies at $T_N \approx 70$ mK and $T_A (T_c) \approx 2$ mK. While the peak at 70 mK illustrates the AF 4f-electronic transition, the one at 2 mK marks the transitions into both nuclear-dominated hybrid AF order (“A phase”) and heavy-fermion superconductivity, as discussed below. A blow-up of the data near the 2 mK-peak at fields below 4 mT indicates that the onset of hybrid order precedes that of superconductivity, with $T_A - T_c$ being less than $0.1T_A$ (Schuberth et al., 2016). **Figure 5B** illustrates how these phase-transition anomalies evolve with increasing magnetic field. The position of the low-temperature anomaly becomes gradually reduced until the latter cannot be resolved anymore above 23 mT, whereas T_N is robust in this whole field range. Clearly resolved is an increase in field-cooled magnetization, $fc-M_{DC}(T)$, upon cooling to below about 20 mK, which indicates a weakening of the staggered magnetization in the primary AF phase. At $T \approx 10$ mK, a significant decrease in the absolute slope of $fc-M_{DC}(T)$ is observed.

Figure 6A displays the zero-field-cooled (zfc-) and $fc-M_{DC}(T)$ curves taken up to $B = 0.418$ mT in a specially shielded setup (different from the one used to obtain the data of **Figure 5**). The data registered at the lowest field, $B = 0.012$ mT, illustrate how the experiment was performed: one starts at $T > 10$ mK by cooling the sample in zero field to the lowest temperature, $T = 0.8$ mK. Then, the field is applied and the zfc curve is recorded on warming to above 10 mK. Cooling again with field applied yields the fc curve. The $zfc-M_{DC}(T)$ curve, which separates abruptly from the fc curve at $T \approx 10$ mK, indicates a shielding signal which is increasing almost linearly upon cooling and assumes a value of not more than 20% just above $T_c = 2$ mK. This is followed by a sharp, pronounced drop at T_c and a robust diamagnetic response at $T \leq 1$ mK. These data are well reproduced by the results of the AC susceptibility obtained under nearly zero-field conditions,

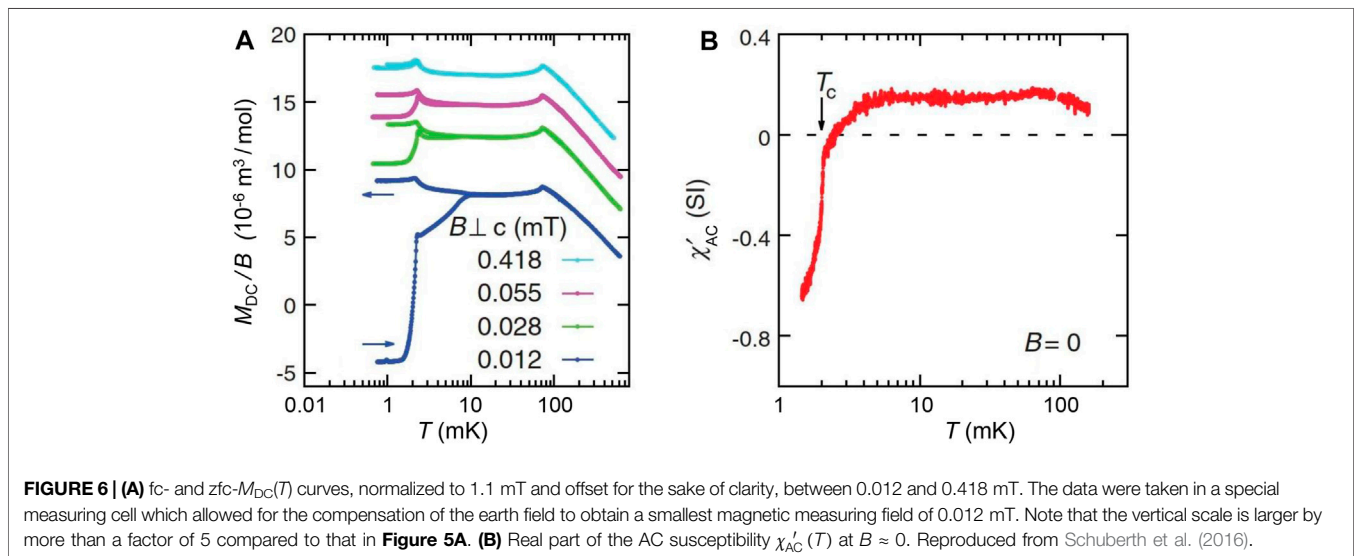
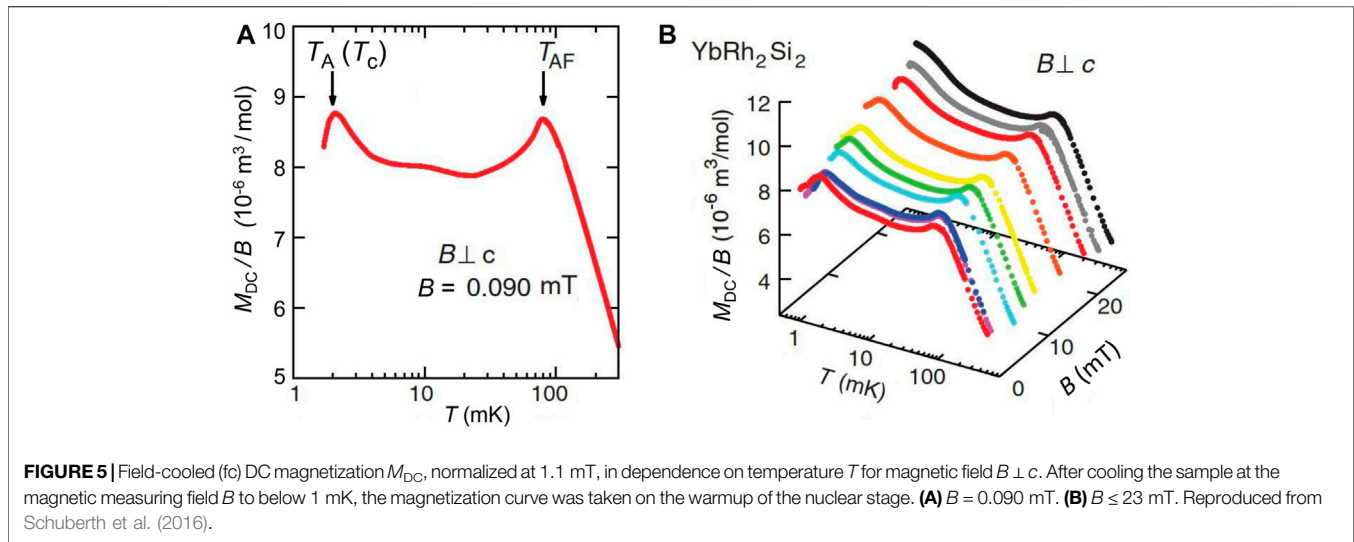
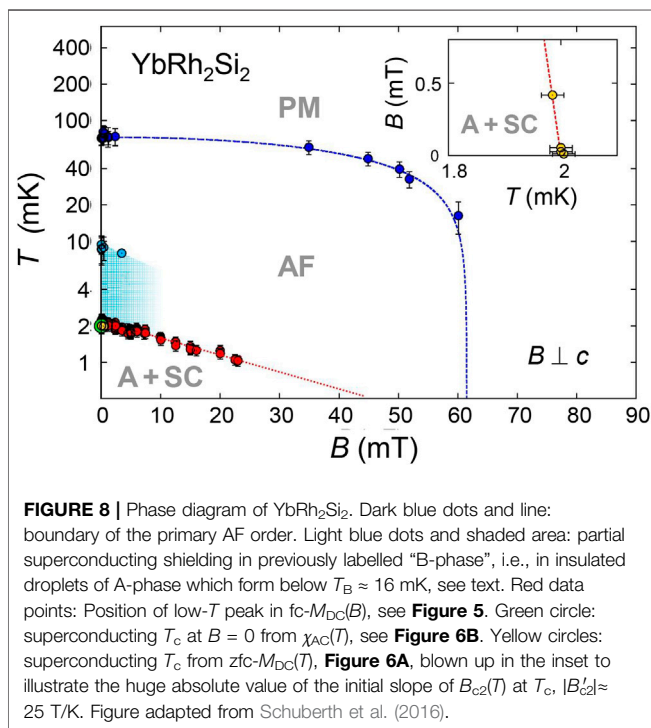
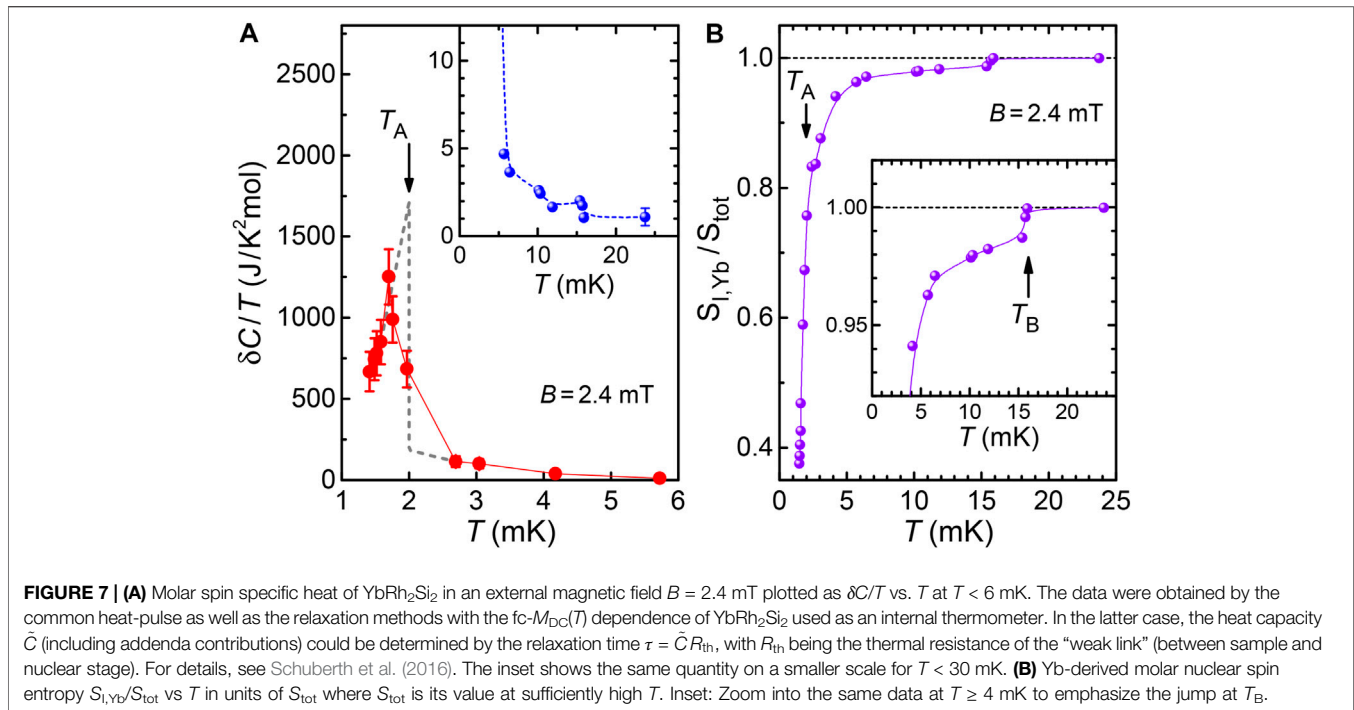


Figure 6B. In the $\chi_{AC}(T)$ data partial shielding below $T \approx 10$ mK and the AF phase transition at $T_N \approx 70$ mK are resolved as well.

We now turn to the peak in the fc- $M_{DC}(T)$ curve at 2 mK which reveals a pronounced decline ΔM of about $0.075 \mu_B$ per Yb down to 0.8 mK (**Figure 5A**). As will be discussed below, about 25% of this decline on the low- T side of the 2 mK-peak should be attributed to the onset of the nuclear-4f electronic hybrid “A-phase”, leaving about 75% of this being due to the Meissner effect. This corresponds to a Meissner volume amounting to only about 2% of the full shielding signal which seems to be quite a small value; however, owing to vortex pinning this is typical for bulk type-II superconductors. After destroying the pinning centers by powdering and subsequent annealing, the sample should exhibit a substantially increased Meissner volume when measured below the lower critical field B_{c1} , see, e.g., Steglich et al. (1979); Rauchschalbe et al. (1982). As also inferred from **Figure 6A**, the shielding signal in zfc- $M_{DC}(T)$ has become

extremely weak at a field as low as 0.418 mT, cf. the discussion below. By contrast, the jump in fc- $M_{DC}(T)$, ΔM , is robust, hinting at the existence of *bulk* superconductivity with $T_c \geq 0.8$ mK up to $B \leq 23$ mT, see **Figure 5B**.

The coefficient of the molar spin specific heat, $\delta C(T)/T$, obtained after subtracting a huge nuclear quadrupolar contribution (for $B = 0$) from the raw data taken at 2.4 mT, is shown below 6 mK in **Figure 7A**. $\delta C(T)$ mainly consists of the contributions by the Yb-derived nuclear spins ($S = 1/2$ for ^{171}Yb ions with a natural abundance of 14.3% as well as $S = 5/2$ for ^{173}Yb ions with 16.1% abundance). Note that neither the ^{100}Rh nor the ^{29}Si nuclear spins contribute to the specific heat above $T = 1$ mK, because they assume their full Zeeman entropies already below this temperature. In addition to the nuclear spin contributions, there is a small one by the 4f-electronic spins, $C_{4f}(T)$. Since the effect of a magnetic field on the nuclear quadrupole contribution is only of higher order, one can use these $\delta C(T)/T$ data, subtracted



by $C_4(T)/T$, to estimate the molar Yb-derived nuclear spin entropy $S_{I,Yb}(T)$ (for $B = 2.4$ mT). Clearly seen in **Figure 7A** is a huge, broadened phase-transition anomaly of mean-field type. The latter can be replaced, under conservation of entropy, by a jump which yields a phase transition temperature of $T_A = 2$ mK

(at $B = 2.4$ mT) and a jump height $\Delta C/T_A$ of ≈ 1700 J/K²mol. This exceeds $\Delta C/T_c$ observed at the transition temperature of typical heavy-fermion superconductors by more than a factor of 1000 and indicates that the A-phase transition is predominantly due to nuclear degrees of freedom. Since an additional measurement at 59.6 mT revealed T_A to be shifted to below the lowest accessible temperature of 0.8 mK, this T_A -anomaly marks the transition into a state of antiferromagnetically ordered nuclear spins. In the inset of **Figure 7A**, $\delta C(T)/T$ is displayed on a largely expanded vertical scale between 6–23 mK, which now contains additional (in comparison to Schuberth et al. (2016)) data for $T > 12$ mK. At $T \geq 18$ mK, where all nuclear spin components are negligible, these data agree well with previous results for $C_4(T)/T$ (Custers et al., 2003), cf. **Figure 2A**. The anomaly visible at $T_B \approx 16$ mK can also be recognized in **Figure 7B**, where the temperature dependence of the entropy of the Yb-derived nuclear spins, $S_{I,Yb}(T)$, is displayed in units of its total (high- T) value, S_{tot} . This anomaly shall be discussed in more detail in the following section.

The temperature-magnetic field phase diagram in **Figure 8** indicates the various low- T , low- B phases of YbRh₂Si₂, i.e., the primary AF phase (blue dots and dashed line), the so-called “B-phase” (light blue shading), the A-phase and superconductivity whose transition temperatures are closely spaced and jointly displayed by the red dots, designating the positions of the low-temperature peaks in fc - $M_{DC}(T)$, see **Figure 5**. The green symbol at $B = 0$ represents the superconducting phase transition observed in $\chi_{AC}(T)$, and the yellow ones, partly hidden by the former, denote the positions of the pronounced shielding signals registered at very low fields by zfc - $M_{DC}(T)$ (**Figure 6A**). These latter transition temperatures are plotted as a function of field in the inset, yielding the absolute initial slope of the upper critical

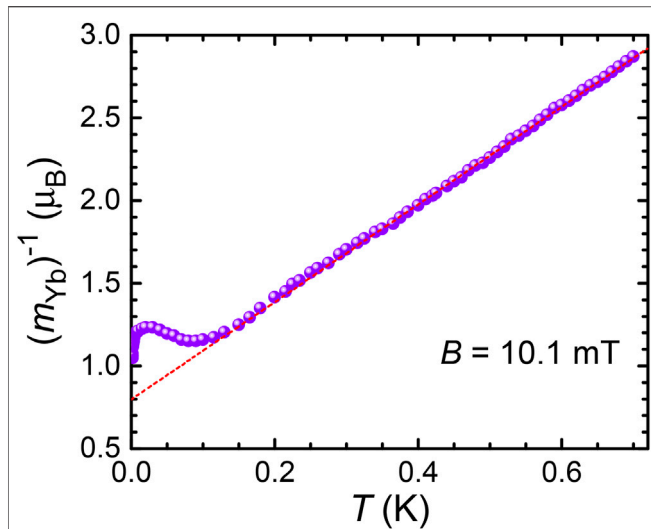


FIGURE 9 | Curie Weiss fit, μ_B/m_{Yb} vs temperature at $B = 10.1$ mT. For $T \rightarrow 0$ a saturation moment $m_{\text{sat}} = 1.24 \mu_B$ is estimated. The Weiss temperature $\theta \approx -0.27$ K agrees well with the result reported by Custers et al. (2003) and illustrates dominant AF correlations at low temperature (Hamann et al., 2019).

field curve at $T = T_c$, $|dB_{c2}(T)/dT| = |B'_{c2}| \approx 25$ T/K. An identical value was obtained from the fc - $M_{DC}(T)$ data at very low fields (Schuberth et al., 2016). The large magnitude of $|B'_{c2}|$ is typical for heavy-fermion superconductors, based upon the ordinary $4f$ -electronic Kondo effect (Assmus et al., 1984). If the giant anomaly in $\delta C(T)/T$ displayed in **Figure 7A** manifested rather a superconducting than a nuclear-ordering transition, one would deal with super-heavy, almost localized, quasiparticles which were originating in a “nuclear Kondo effect” (Coleman, 2015). In this case, the spins of the conduction electrons would rather screen the Yb-derived nuclear than the $4f$ -electronic spins. This scenario cannot be at play as it would result in an almost infinite slope $|B'_{c2}|$.

One can derive the effective g -factor of the A-phase, $g_{\text{eff}} \approx 0.051$, from the ratio of the transition temperature $T_A(B = 0) = 2.3$ mK and the critical field $B_A(T \rightarrow 0) \approx 45$ mT (**Figure 8**). Using the in-plane $4f$ - g -factor of YbRh₂Si₂, $g_{4f} = 3.5$ (Sichelschmidt et al., 2003), one finds the A-phase to represent hybrid AF order comprising a dominant ($\approx 98.5\%$) nuclear component and a tiny $4f$ -electronic component of $\approx 1.5\%$, with a staggered moment of $m_f \approx 0.018 \mu_B$. This is obtained with the aid of the ($T \rightarrow 0$) saturation moment, $1.24 \mu_B$, as estimated from a Curie-Weiss fit to the fc -magnetization data taken in the paramagnetic regime at

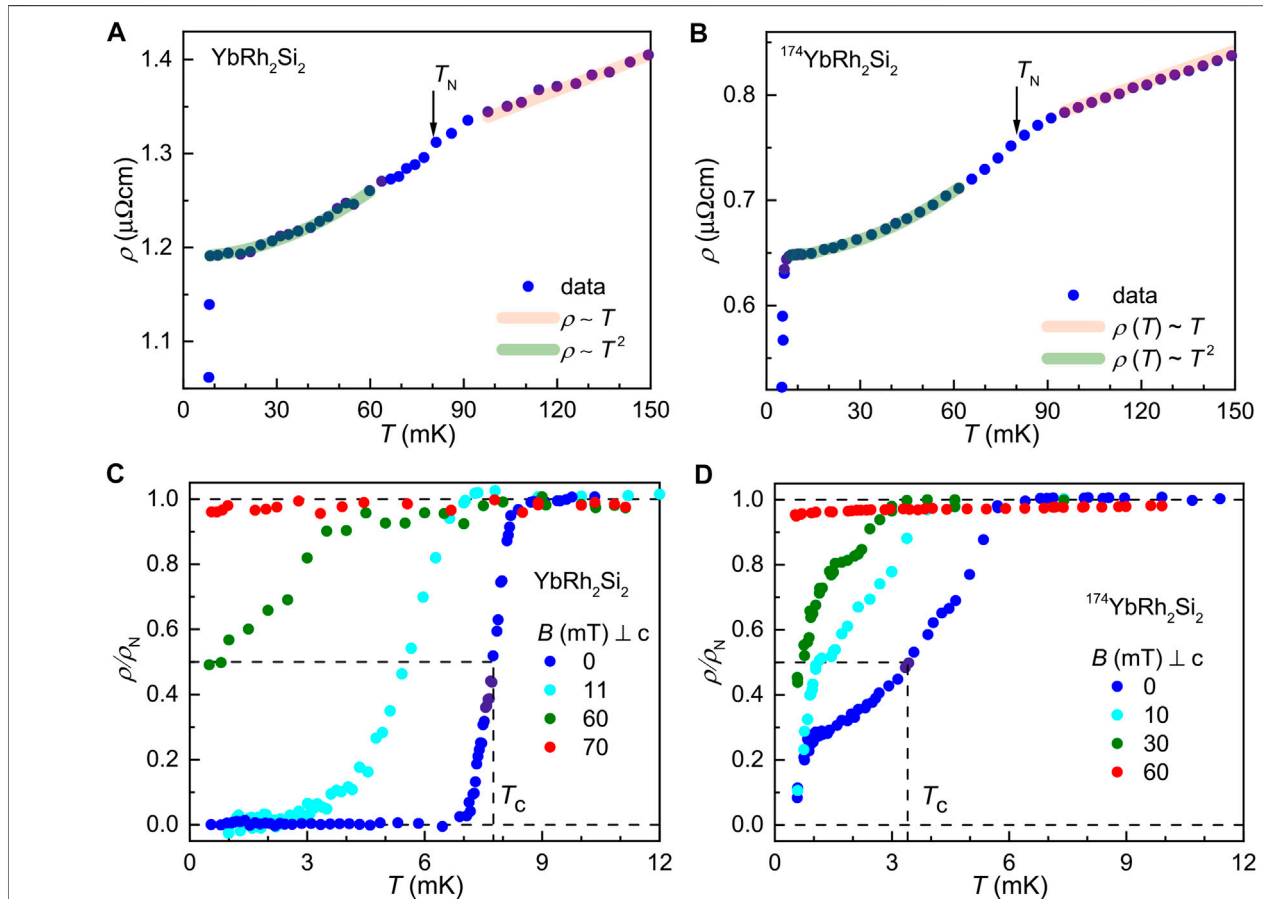


FIGURE 10 | Electrical resistivity as a function of temperature for **(A), (C)** YbRh₂Si₂ and **(B), (D)** ¹⁷⁴YbRh₂Si₂ at $B = 0$ and various applied fields. Reproduced from Nguyen et al. (2021) under a Creative Commons Attribution 4.0 International License. Copyright 2021, The Authors, published by Springer Nature.

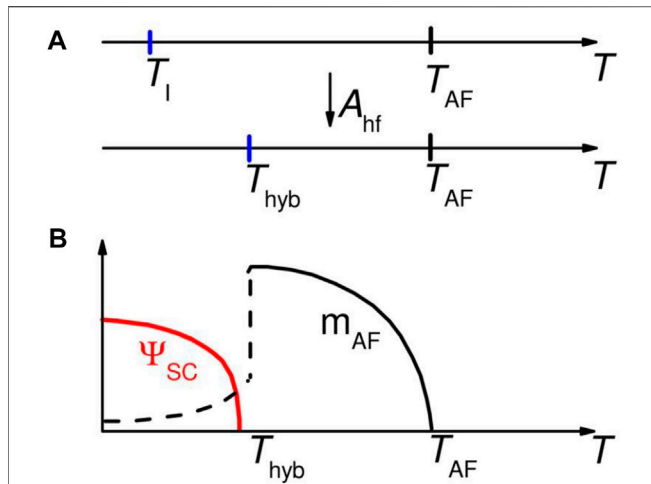


FIGURE 11 | Three component Landau theory: Phase transitions at T_{AF} and T_{hyb} . **(A)** Sketch of the two phase transitions associated with electronic and nuclear spin orders. (Top line) Without any hyperfine coupling (A_{hf}), the electronic and nuclear spins are ordered at T_{AF} and T_I , respectively. (Bottom line) With hyperfine coupling, T_{AF} is not affected, but a hybrid nuclear and electronic spin order is induced at $T_{hyb} > T_I$. **(B)** Temperature evolution of the primary electronic spin order parameter (m_{AF}) and the superconducting order parameter Ψ_{SC} . Ψ_{SC} is developed when m_{AF} is suppressed by the formation of hybrid nuclear and electronic spin order directly below T_{hyb} . Reproduced from Schuberth et al. (2016).

an external field of 10.1 mT, see **Figure 9**. The staggered moment m_j exceeds significantly that of the primary AF phase, $m_{AF} \approx 0.002 \mu_B$ (Ishida et al., 2003) which may explain the “re-entrant AF order” at very low temperatures as reported by Saunders (2018) based on measurements of Nyquist noise. We note that a pure nuclear phase transition would not be resolved in our magnetization measurements because of the very small nuclear moment. Therefore, one can state that the 2 mK-peak in $fc-M_{DC}(T)$ originates in the tiny $4f$ -component of the hybrid A-phase (and additionally, to a larger part in the Meissner signal of the superconducting transition), while the huge anomaly in the specific-heat coefficient shown in **Figure 7A** is only due to the Yb-derived nuclear spin states. We infer from the red data points shown in **Figure 8** and the results of **Figure 5B** that the existence range for bulk superconductivity is most likely extended to fields in excess of 23 mT where the values of T_c are below 0.8 mK.

Measurements of the electrical resistivity at ultra-low temperatures are extremely difficult in view of the unavoidable contact resistances which may easily heat up the sample. Recently, Nguyen et al. were successful in performing such measurements on YbRh₂Si₂ single crystals down to 0.5 mK (Nguyen et al., 2021). **Figure 10** reproduces their results on a pristine sample of YbRh₂Si₂ (A, C) as well as on a single crystal with nominally 100 at% of ¹⁷⁴Yb ions which do not carry nuclear spins (denoted as ¹⁷⁴YbRh₂Si₂ in B, D). This latter sample had been prepared and intensively studied by Knebel et al. (2006). For both single crystals the onset of the primary AF order at $T_N = 70$ mK is resolved, see **Figures 10A,B**, as is the superconducting transition with a (mid-point) $T_c = 7.9$ mK,

following an onset at ≈ 9 mK for the YbRh₂Si₂ crystal and an onset at about 5 mK for the ¹⁷⁴YbRh₂Si₂ crystal (**Figures 10C,D**). Within the resolution of the experiments, the resistivity reaches $\rho = 0$ at about 6.5 mK for the former sample (**Figure 10C**). In case of the nominally nuclear-spin free ¹⁷⁴YbRh₂Si₂ sample, the onset of superconductivity at 5 mK is followed by a broadened 75% decrease of $\rho(T)$, which starts to decline in a substantially steeper fashion at about 1 mK, without reaching zero at the low- T limit of 0.5 mK, suggesting $\rho = 0$ at around 0.3–0.4 mK (**Figure 10D**). Under external magnetic field the transitions are shifted to lower temperatures. As shown in **Figure 10C**, for the YbRh₂Si₂ sample, the transition is broadened at $B = 11$ mT, and zero resistivity is achieved at $T \approx 2$ mK. Even at $B = 60$ mT a residual, very broad and incomplete transition is recognized. The initial $T_c(B)$ dependence is found to be relatively steep, implying an absolute initial slope of $|B'_{c2}| \approx 4.4$ T/K. The field dependence of T_c becomes flatter above $B \approx 11$ mT. The finite-field data for the ¹⁷⁴YbRh₂Si₂ sample displayed in **Figure 10D** show a field-induced reduction of the temperature range of the broad initial decline in $\rho(T)$. In addition, the temperature of 0.3–0.4 mK at which $\rho(T)$ is likely to vanish, appears to be almost independent of field up to $B = 30$ mT.

To put these new results in perspective, we wish to note that resistive transitions (at $T_{c,\rho}$) commonly probe percolative superconductivity, with $\rho(T)$ reaching zero when the first percolating path through the sample is formed. On the other hand, both $\chi_{AC}(T)$ (with $T_{c,\chi}$) and $zfc-M_{DC}(T)$ provide shielding signals due to “networks of screening currents” in the sample surface. The thermodynamic (bulk-) T_c is obtained through transitions in the specific heat and/or the Meissner effect as measured by $fc-M_{DC}(T)$ (with $T_{c,M}$). For inhomogeneous superconductors one frequently finds $T_{c,\rho} > T_{c,\chi} > T_{c,M}$. In case of the Ce-based 115-superconductors with anisotropic transport owing to the delicate interplay of competition and coexistence between superconductivity and AF order, an exotic type of percolative (“textured”) superconductivity has been reported (Park et al., 2012). For CeIrIn₅, the thermodynamic T_c probed via specific heat is 0.4 K, while $T_{c,\rho} = 1.2$ K (Petrovic et al., 2001).

In the YbRh₂Si₂ sample, the onset of superconductivity at very low fields is observed at almost the same $T_{c,\rho} \approx 8$ mK in measurements of both the electrical resistivity (Nguyen et al., 2021) and Nyquist noise (Saunders, 2018). In this exceptional case $T_{c,\rho}$, and even the onset temperature of the resistive transition, is smaller than $T_{c,\chi} \approx 10$ mK. The resistivity study yields an absolute initial slope of $B_{c2}(T)$ at T_c , $|B'_{c2}| \approx 4.4$ T/K discussed above, which is much smaller than the value 25 T/K based on zfc - and $fc-M_{DC}(T)$ results, cf. the preceding **Section 2**. In addition, the thermodynamic superconducting transition displayed by the low-temperature peak in $fc-M_{DC}(T)$ is corroborated by abrupt and large shielding signals in both $zfc-M_{DC}(T)$ and $\chi_{AC}(T)$, cf. **Figures 6A,B**, respectively.

Concerning the ¹⁷⁴YbRh₂Si₂ sample, we believe that 1) it contains a low, but finite, concentration of residual Yb ions with nuclear spins which give rise to a weakened hybrid A-phase order and, thus, weakened superconductivity, and 2) YbRh₂Si₂ free of nuclear spins would not be a superconductor, at least near $B = 0$. To check this, future studies of superconductivity of YbRh₂Si₂ samples with enriched ¹⁷⁴Yb isotope should be assisted by high-precision mass

spectrometry, which is required to determine the amount of residual nuclear spins.

A three-component Landau theory was applied in Schuberth et al. (2016) to explain the development of two subsequent AF phase transitions at T_N and T_A . (Assuming two components, one would obtain only one phase transition). This theoretical treatment was based on the empirical knowledge that the 4f-electronic spin susceptibility $\chi_{4f}(\mathbf{Q})$ is highly anisotropic, exhibiting maxima at two wave vectors, \mathbf{Q}_{AF} and $\mathbf{Q} = 0$, and giving rise to the primary AF order and ferromagnetic correlations (Gegenwart et al., 2005), respectively.

It is, therefore, natural to assume that a peak in $\chi_{4f}(\mathbf{Q})$ exists at yet another finite wave vector \mathbf{Q}_1 , different from \mathbf{Q}_{AF} . Along \mathbf{Q}_1 , the RKKY interaction generates an order parameter Φ_j among the 4f-electronic spins and simultaneously an order parameter Φ_I among the Yb-derived nuclear spins. According to the size of the effective g -factor discussed above, Φ_I must be much larger than Φ_j . As Φ_j and Φ_I exist at the same wave vector \mathbf{Q}_1 , they are coupled bilinearly via $-\lambda \Phi_j \Phi_I$, where the coupling parameter $\lambda \approx 25$ mK is related to the hyperfine coupling constant A_{hf} by $\lambda \sim A_{hf} \approx 100$ T/ μ_B . As a result, one finds the transition temperature of the nuclear-dominated hybrid A-phase $T_{hyb} \approx \lambda^2 \chi_{4f}(\mathbf{Q}_1)/g_{4f}^2 \approx 1$ mK. Here, the value of the bulk susceptibility was taken for that of the unknown $\chi_{4f}(\mathbf{Q}_1)$. In view of this uncertainty, the agreement between the theoretical result for T_{hyb} and the experimental value $T_A = 2$ mK is surprisingly good. Within the afore-described Landau treatment it may be assumed that the nuclear order parameter Φ_I competes with the primary 4f-electronic order parameter Φ_{AF} that was found to be detrimental to superconductivity. Consequently, superconductivity sets in once the primary order Φ_{AF} is suppressed, cf. **Figure 11**.

As this Landau theory is a mean-field theory, it does not treat short-range order. However, unique nuclear short-range order, as visualized by a significant temperature dependence of the nuclear spin entropy (**Figure 7B**), apparently exists up to at least 16 mK and generates the nucleation of superconductivity at $T \approx 10$ mK (**Figure 6A**). In reality, as was inferred from **Figure 5A**, the staggered magnetization of the primary AF phase, m_{AF} , starts to decrease already at 20 mK, rather than at $T = T_{hyb}$. As suggested in **Figure 11**, $m_{AF}(T)$ continues to decrease below T_{hyb} and may well vanish as $T \rightarrow 0$. This means, the QCP is located at (or very close to) zero external magnetic field. Interestingly, the transition from the primary AF order to superconductivity is of first order (Schuberth et al., 2016), similar to what was found for single-crystalline A/S-type CeCu₂Si₂ (Stockert et al., 2006a).

In the following we summarize, and offer a—possibly oversimplified—explanation of, the multitude of puzzling results achieved by the previous magnetic and calorimetric as well as the recent resistive measurements:

- 1) Superconductivity in YbRh₂Si₂ apparently exists in a wide field range almost up to $B_A = 45$ mT, with the maximum T_c occurring at $B = 0$ (Schuberth et al., 2016).
- 2) The T -dependence of $fc-M_{DC}(T)$ displayed in **Figure 5A** demonstrates that the staggered moment, m_{AF} , of the

primary order starts to decrease already at about 20 mK, which is close to the temperature associated with the strength of the local Yb hyperfine interaction (25 mK). In addition, a significant T -dependence of the Yb-derived nuclear spin entropy, $S_{I,Yb}(T)$, is observed up to $T_B \approx 16$ mK, where a distinct anomaly is visible in **Figure 7**. The latter is associated with a rather sharp removal of a tiny fraction of about 1.5% of S_{tot} , the full value of $S_{I,Yb}(T)$ at high temperatures. This can be ascribed to a corresponding small fraction of the Yb-derived nuclear spins which interact with the mean hyperfine field induced by the 4f-electron spins (Schuberth et al., 2016) to create random and insulated A-phase regions which must be growing upon lowering the temperature.

- 3) The simultaneous onset of both a weak, but distinct shielding signal (**Figure 6**) and a pronounced decline in the absolute slope of $fc M_{DC}(T)$ (**Figure 5A**) at $T \approx 10$ mK are interpreted as manifesting the nucleation of superconductivity.
- 4) The network of superconducting islands turns out to be extremely fragile as the shielding signal is suppressed already by a very small external magnetic field (**Figure 6A**).
- 5) Upon further cooling, the resistivity reaches zero at about 6.5 mK. This can be reconciled with the above results in terms of the onset of superconducting percolation as mentioned before. The percolation initiates a considerably increasing strength of A-phase short-range order as illustrated by a pronounced increase of $fc-M_{DC}(T)$ below 5 mK (**Figure 5A**) and corroborated by a significant removal of the Yb-derived nuclear spin entropy from its maximum value S_{tot} (at $T > T_B$) by 26% on cooling the sample down to T_A (**Figure 7B**). Remarkably, the shielding signal due to the network of superconducting islands in the sample surface does not exceed 20% when cooling from $T \approx 10$ mK to $T \geq T_A$, the temperature range previously called “B-phase”, cf. **Figure 8**.
- 6) At $T_A (= 2.3$ mK as $B \rightarrow 0$, see Schuberth et al. (2016)), a second-order phase transition into long-range A-phase order takes place (**Figure 7A**). The ordering of the Yb nuclear spins reaches a level of more than 60% already at 1.5 mK, see **Figure 7B**. Nuclear-dominated hybrid order at elevated magnetic fields has yet to be confirmed by future measurements of the specific heat. This should clarify whether the A-phase exists up to $B_A \approx 45$ mT, as indicated by the dotted red line in the phase diagram of **Figure 8**, or even up to the quantum critical field $B_N = 60$ mT, as suggested by the new resistivity results of Nguyen et al. (2021), **Figure 10**. In the latter case, we conjecture the existence of not just two QCPs at $B = B_N$ (vanishing of the primary AF order due to the applied magnetic field) and at $B = 0$ (due to the competing A-phase). Rather, a phase boundary $T_A(B)$ spanning the whole field range $B < B_N$ would exist and most likely establish a *quantum critical line* between these two QCPs.
- 7) From the magnetization measurements (Schuberth et al., 2016), bulk superconductivity emerges at $T_c = 2$ mK (**Figures 5A, 6A**), slightly below T_A . Future $fc-M_{DC}(T)$ measurements on annealed powder samples below the lower critical field B_{c1} are needed to confirm that bulk superconductivity indeed exists well below $T_{c,\rho}$ at magnetic fields up to $B \approx B_A$.

We should welcome future work by other groups to cross-check the above reasoning.

The new resistivity study by Nguyen et al. (2021) suggests the existence of two separate superconducting regimes, at low and elevated fields, respectively. In view of the preceding discussion, we cannot concur with the proposal by Nguyen et al. that, at least in the low-field regime, Cooper pairing in YbRh₂Si₂ is mediated by the critical fluctuations of the *field-induced* QCP at B_N : For, here the primary AF order is apparently suppressed by the competing nuclear order, allowing a quantum critical line to be established. Therefore, it is natural to consider the associated quantum critical fluctuations at *very low fields* being the driving force for the formation of Cooper pairs.

The origin of the superconductivity at elevated fields remains to be resolved. If here, the existence of the nuclear-dominated hybrid A-phase can be proven by future specific-heat experiments, the Cooper-pairing mechanism emphasized above in the low-field regime will most likely be operating as well. An alternative scenario proposed by Nguyen et al. (2021) neglects the competition between the nuclear and primary *4f*-electronic orders and instead implies, as mentioned before, that the quantum critical fluctuations associated with the *field-induced* QCP at $B_N = 60$ mT bring about the formation of superconductivity. As these critical fluctuations would be strongly impeded by the pair-breaking applied magnetic field, the competition between the field-induced quantum criticality and the destructive action of the magnetic field on the Cooper pairs causes a maximum T_c to occur well below B_N . Nguyen et al. (2021) propose that superconductivity at elevated field may be of the spin-triplet variety. While this would not have been a surprise had the quantum criticality been of nearly ferromagnetic (and conventional) type (Li et al., 2019), how could spin-triplet pairing develop for Kondo-destroying type AF quantum criticality as is the case in YbRh₂Si₂? Insights into this question have come from theoretical studies near a Kondo-destroying QCP in antiferromagnetically coupled Kondo models (Hu et al., 2021b): They showed that significant Ising anisotropy, as it effectively arises under an external magnetic field in the easy-plane antiferromagnetically correlated YbRh₂Si₂, makes the spin-triplet pairing competitive.

3 PERSPECTIVE

The discovery of superconductivity in YbRh₂Si₂ at ultra-low temperatures opens up new dimensions. It expands the horizon of ultra-low temperature physics towards strongly correlated electronic matter in solids and conversely, it determines a new area of heavy-fermion physics by reaching down to ultra-low temperatures.

Up to now, heavy-fermion superconductivity has been detected in more than fifty *f*-electron compounds. Despite the fact that, compared with PuCoGa₅, exhibiting the record-high T_c of 18.5 K (Sarrao et al., 2002), YbRh₂Si₂ shows a transition temperature which is lower by almost four decades, this may be called “high T_c ”—in the sense that T_c is limited by an enormously high ordering temperature of nuclear spins. This nuclear order paves the way for the superconductivity, not by actively helping in the Cooper-pair formation, rather by destroying the *4f*-electronic order below $T_N = 70$ mK, which appears to be extremely hostile to superconductivity. The apparent competition between the nuclear and the *4f*-electronic orders results in an AF QCP at, or very close to, $B = 0$. Most likely, the latter—like its field-induced counterpart at $B = B_N$ —is of the “local” type, as inferred from the $B = 0$ results of electrical and thermal transport as well as specific-heat measurements in the paramagnetic state as presented in **Section 1**.

The ultra-low temperature work on YbRh₂Si₂ strongly supports the notion that superconductivity robustly develops in the vicinity of such a “partial-Mott” QCP, as has been theoretically derived in Kondo-lattice models for a Kondo-destroying QCP (Hu et al., 2021a) and experimentally evidenced from de Haas-van Alphen studies in high magnetic fields (Shishido et al., 2005) and transport measurements (Park et al., 2006) on pressurized CeRhIn₅. Therefore, the results on these two compounds provide the long-sought (Maple et al., 2004) link between unconventional superconductivity in heavy-fermion metals (Pfleiderer, 2009) and that occurring near a true Mott metal-insulator transition, e.g., in the cuprates (Lee et al., 2006) and organic charge-transfer salts (Kanoda, 2008).

AUTHOR CONTRIBUTIONS

All authors listed have made a substantial, direct, and intellectual contribution to the work and approved it for publication.

FUNDING

SW acknowledges support by the Deutsche Forschungsgemeinschaft through WI 1324/5-1.

ACKNOWLEDGMENTS

We are grateful for conversations with Manuel Brando, Ang Cai, Lei Chen, Piers Coleman, Haoyu Hu, Stefan Lausberg, Silke Paschen, John Saunders, Rong Yu and in particular Qimiao Si for his insightful comments.

REFERENCES

- Alexandrov, V., Coleman, P., and Erten, O. (2015). Kondo Breakdown in Topological Kondo Insulators. *Phys. Rev. Lett.* 114, 177202. doi:10.1103/physrevlett.114.177202
- Aronson, M. C., Osborn, R., Robinson, R. A., Lynn, J. W., Chau, R., Seaman, C. L., et al. (1995). Non-Fermi-Liquid Scaling of the Magnetic Response in UCu_{5-x}Pd_x(x=1,1.5). *Phys. Rev. Lett.* 75, 725–728. doi:10.1103/physrevlett.75.725
- Assmus, W., Herrmann, M., Rauchschalbe, U., Riegel, S., Lieke, W., Spille, H., et al. (1984). Superconductivity in CeCu₂Si₂ Single Crystals. *Phys. Rev. Lett.* 52, 469–472. doi:10.1103/physrevlett.52.469
- Chen, Q. Y., Xu, D. F., Niu, X. H., Peng, R., Xu, H. C., Wen, C. H. P., et al. (2018). Band Dependent Interlayer *f*-Electron Hybridization in CeRhIn₅. *Phys. Rev. Lett.* 120, 066403. doi:10.1103/PhysRevLett.120.066403
- Chen, Q. Y., Xu, D. F., Niu, X. H., Jiang, J., Peng, R., Xu, H. C., et al. (2017). Direct Observation of How the Heavy-Fermion State Develops in CeCoIn₅. *Phys. Rev. B* 96, 045107. doi:10.1103/physrevb.96.045107
- Coleman, P., Anderson, P. W., and Ramakrishnan, T. V. (1985). Theory for the Anomalous Hall Constant of Mixed-Valence Systems. *Phys. Rev. Lett.* 55, 414–417. doi:10.1103/physrevlett.55.414
- Coleman, P., Pépin, C., Si, Q., and Ramazashvili, R. (2001). How Do Fermi liquids get heavy and die? *J. Phys. Condens. Matter* 13, R723–R738. doi:10.1088/0953-8984/13/35/202
- Coleman, P. (2015). *Private Communication*.
- Custers, J., Gegenwart, P., Wilhelm, H., Neumaier, K., Tokiwa, Y., Trovarelli, O., et al. (2003). The Break-Up of Heavy Electrons at a Quantum Critical Point. *Nature* 424, 524–527. doi:10.1038/nature01774
- Dong, J. K., Tokiwa, Y., Bud'ko, S. L., Canfield, P. C., and Gegenwart, P. (2013). Anomalous Reduction of the Lorenz Ratio at the Quantum Critical Point in YbAgGe. *Phys. Rev. Lett.* 110, 176402. doi:10.1103/physrevlett.110.176402
- Ernst, S., Kirchner, S., Krellner, C., Geibel, C., Zwicky, G., Steglich, F., et al. (2011). Emerging Local Kondo Screening and Spatial Coherence in the Heavy-Fermion Metal YbRh₂Si₂. *Nature* 474, 362–366. doi:10.1038/nature10148
- Friedemann, S., Oeschler, N., Wirth, S., Krellner, C., Geibel, C., Steglich, F., et al. (2010). Fermi-Surface Collapse and Dynamical Scaling Near a Quantum-Critical Point. *Proc. Natl. Acad. Sci. U.S.A.* 107, 14547–14551. doi:10.1073/pnas.1009202107
- Gegenwart, P., Custers, J., Geibel, C., Neumaier, K., Tayama, T., Tenya, K., et al. (2002). Magnetic-field Induced Quantum Critical Point in YbRh₂Si₂. *Phys. Rev. Lett.* 89, 056402. doi:10.1103/physrevlett.89.056402
- Gegenwart, P., Custers, J., Tokiwa, Y., Geibel, C., and Steglich, F. (2005). Ferromagnetic Quantum Critical Fluctuations in YbRh₂(Si_{0.95}Ge_{0.05})₂. *Phys. Rev. Lett.* 94, 076402. doi:10.1103/physrevlett.94.076402
- Gegenwart, P., Westerkamp, T., Krellner, C., Tokiwa, Y., Paschen, S., Geibel, C., et al. (2007). Multiple Energy Scales at a Quantum Critical Point. *Science* 315, 969–971. doi:10.1126/science.1136020
- Gegenwart, P., Si, Q., and Steglich, F. (2008). Quantum Criticality in Heavy-Fermion Metals. *Nat. Phys.* 4, 186–197. doi:10.1038/nphys892
- Hamann, S., Zhang, J., Jang, D., Hannaske, A., Steinke, L., Lausberg, S., et al. (2019). Evolution from Ferromagnetism to Antiferromagnetism in Yb(Rh_{1-x}Co_x)₂Si₂. *Phys. Rev. Lett.* 122, 077202. doi:10.1103/physrevlett.122.077202
- Hartmann, S., Oeschler, N., Krellner, C., Geibel, C., Paschen, S., and Steglich, F. (2010). Thermopower Evidence for an Abrupt Fermi Surface Change at the Quantum Critical Point of YbRh₂Si₂. *Phys. Rev. Lett.* 104, 096401. doi:10.1103/physrevlett.104.096401
- Hu, H., Cai, A., Chen, L., Deng, L., Pixley, J. H., Ingersent, K., et al. (2021a). Unconventional Superconductivity from Fermi Surface Fluctuations in Strongly Correlated Metals. *arXiv:2109.13224*.
- Hu, H., Cai, A., Chen, L., and Si, Q. (2021b). Spin-Singlet and Spin-Triplet Pairing Correlations in Antiferromagnetically Coupled Kondo Systems. *arXiv:2109.12794*.
- Ishida, K., MacLaughlin, D. E., Young, B.-L., Okamoto, K., Kawasaki, Y., Kitaoka, Y., et al. (2003). Low-temperature Magnetic Order and Spin Dynamics in YbRh₂Si₂. *Phys. Rev. B* 68, 184401. doi:10.1103/physrevb.68.184401
- Kanoda, K. (2008). “Mott Transition and Superconductivity in quasi-2D Organic Conductors,” in *The Physics of Organic Superconductors and Conductors*. Editor A. Lebed (Berlin, Heidelberg: Springer-Verlag), 623–642. doi:10.1007/978-3-540-76672-8_22
- Kirchner, S., Paschen, S., Chen, Q., Wirth, S., Feng, D., Thompson, J. D., et al. (2020). Heavy Electron Quantum Criticality and Single-Particle Spectroscopy. *Rev. Mod. Phys.* 92, 011002. doi:10.1103/revmodphys.92.011002
- Knebel, G., Boursier, R., Hassinger, E., Lapertot, G., G. Niklowitz, P., Pourret, A., et al. (2006). Localization of 4*f* State in YbRh₂Si₂ under Magnetic Field and High Pressure: Comparison with CeRh₂Si₂. *J. Phys. Soc. Jpn.* 75, 114709. doi:10.1143/jpsj.75.114709
- Köhler, U., Oeschler, N., Steglich, F., Maquilon, S., and Fisk, Z. (2008). Energy Scales of Lu_{1-x}Yb_xRh₂Si₂ by Means of Thermopower Investigations. *Phys. Rev. B* 77, 104412.
- Lausberg, S. (2013). *Quantum Criticality in Ferromagnetic Correlated Ce- and Yb-Based Heavy Fermion Systems (In German)* (Germany: Technical University Dresden). Ph.D. thesis.
- Lee, P. A., Nagao, N., and Wen, X.-G. (2006). Doping a Mott Insulator: Physics of High-Temperature Superconductivity. *Rev. Mod. Phys.* 78, 17–85. doi:10.1103/revmodphys.78.17
- Li, Y., Wang, Q., Xu, Y., Xie, W., and Yang, F. Y. (2019). Nearly Degenerate *p_x + ip_y* and *d_{x²-y²}* Pairing Symmetry in the Heavy Fermion Superconductor YbRh₂Si₂. *Phys. Rev. B* 100, 085132. doi:10.1103/physrevb.100.085132
- Machida, Y., Tomokuni, K., Izawa, K., Lapertot, G., Knebel, G., Brison, J.-P., et al. (2013). Verification of the Wiedemann-Franz Law in YbRh₂Si₂ at a Quantum Critical Point. *Phys. Rev. Lett.* 110, 236402. doi:10.1103/physrevlett.110.236402
- Maple, M. B., Bauer, E. D., Zapf, V. S., and Wosnitza, J. (2004). “Unconventional Superconductivity in Novel Materials,” in *The Physics of Superconductors*. Editors K. H. Bennemann and J. B. Ketterson (Berlin, Heidelberg: Springer), II, 555–730. doi:10.1007/978-3-642-18914-2_8
- Nguyen, D. H., Sidorenko, A., Taupin, M., Knebel, G., Lapertot, G., Schuberth, E., et al. (2021). Superconductivity in an Extreme Strange Metal. *Nat. Commun.* 12, 4341. doi:10.1038/s41467-021-24670-z
- Parfen'eva, L. S., Smirnov, I. A., Misiorek, H., Mucha, J., Jezowski, A., Prokofev, A. V., et al. (2004). Spinon Thermal Conductivity of (CuO₂)-Spin Chains in LiCuVO₄. *Phys. Solid State.* 46, 357–363. doi:10.1134/1.1649437
- Park, T., Lee, H., Martin, I., Lu, X., Sidorov, V. A., Gofryk, K., et al. (2012). Textured Superconducting Phase in the Heavy Fermion CeRhIn₅. *Phys. Rev. Lett.* 108, 077003. doi:10.1103/PhysRevLett.108.077003
- Park, T., Ronning, F., Yuan, H. Q., Salamon, M. B., Movshovich, R., Sarrao, J. L., et al. (2006). Hidden Magnetism and Quantum Criticality in the Heavy Fermion Superconductor CeRhIn₅. *Nature* 440, 65–68. doi:10.1038/nature04571
- Paschen, S., Lühmann, T., Wirth, S., Gegenwart, P., Trovarelli, O., Geibel, C., et al. (2004). Hall-effect Evolution across a Heavy-Fermion Quantum Critical Point. *Nature* 432, 881–885. doi:10.1038/nature03129
- Petrovic, C., Movshovich, R., Jaime, M., Pagliuso, P. G., Hundley, M. F., Sarrao, J. L., et al. (2001). A New Heavy-Fermion Superconductor CeIrIn₅: A Relative of the Cuprates? *Europhys. Lett.* 53, 354–359. doi:10.1209/epl/i2001-00161-8
- Pfau, H., Hartmann, S., Stockert, U., Sun, P., Lausberg, S., Brando, M., et al. (2012). Thermal and Electrical Transport across a Magnetic Quantum Critical Point. *Nature* 484, 493–497. doi:10.1038/nature11072
- Pfleiderer, C. (2009). Superconducting Phases of *f*-Electron Compounds. *Rev. Mod. Phys.* 81, 1551–1624. doi:10.1103/revmodphys.81.1551
- Pourret, A., Aoki, D., Boukahil, M., Brison, J.-P., Knafo, W., Knebel, G., et al. (2014). Quantum Criticality and Lifshitz Transition in the Ising System CeRu₂Si₂: Comparison with YbRh₂Si₂. *J. Phys. Soc. Jpn.* 83, 061002. doi:10.7566/jpsj.83.061002
- Rauchschalbe, U., Lieke, W., Bredl, C. D., Steglich, F., Aarts, J., Martini, K. M., et al. (1982). Critical Fields of the “Heavy-Fermion” Superconductor CeCu₂Si₂. *Phys. Rev. Lett.* 49, 1448–1451. doi:10.1103/physrevlett.49.1448
- Reid, J.-P., Tanatar, M. A., Daou, R., Hu, R., Petrovic, C., and Taillefer, L. (2014). Wiedemann-Franz Law and Non-Vanishing Temperature Scale across the Field-Tuned Quantum Critical Point of YbRh₂Si₂. *Phys. Rev. B* 89, 045130. doi:10.1103/physrevb.89.045130
- Sachdev, S. (2011). *Quantum Phase Transitions*. Cambridge, England: Cambridge University Press.

- Sarrao, J. L., Morales, L. A., Thompson, J. D., Scott, B. L., Stewart, G. R., Wastin, F., et al. (2002). Plutonium-based Superconductivity with a Transition Temperature above 18 K. *Nature* 420, 297–299. doi:10.1038/nature01212
- Saunders, J. (2018). “Superconductivity in YbRh₂Si₂: Electrical Transport and Noise Experiments,” in Invited Talk at 12th Intern. Conf. on Materials and Mechanisms of Superconductivity (M2S 2018), Beijing, China, August 19–24, 2018.
- Schröder, A., Aeppli, G., Coldea, R., Adams, M., Stockert, O., v. Löhneysen, H., et al. (2000). Onset of Antiferromagnetism in Heavy-Fermion Metals. *Nature* 407, 351–355. doi:10.1038/35030039
- Schuberth, E., Tippmann, M., Steinke, L., Lausberg, S., Steppke, A., Brando, M., et al. (2016). Emergence of Superconductivity in the Canonical Heavy-Electron Metal YbRh₂Si₂. *Science* 351, 485–488. doi:10.1126/science.aaa9733
- Seiro, S., Jiao, L., Kirchner, S., Hartmann, S., Friedemann, S., Krellner, C., et al. (2018). Evolution of the Kondo Lattice and Non-Fermi Liquid Excitations in a Heavy-Fermion Metal. *Nat. Commun.* 9, 3324. doi:10.1038/s41467-018-05801-5
- Shishido, H., Settai, R., Harima, H., and Ōnuki, Y. (2005). A Drastic Change of the Fermi Surface at a Critical Pressure in CeRhIn₅: dHvA Study under Pressure. *J. Phys. Soc. Jpn.* 74, 1103–1106. doi:10.1143/jpsj.74.1103
- Si, Q., Rabello, S., Ingersent, K., and Smith, J. L. (2001). Locally Critical Quantum Phase Transitions in Strongly Correlated Metals. *Nature* 413, 804–808. doi:10.1038/35101507
- Sichelschmidt, J., Ivanshin, V. A., Ferstl, J., Geibel, C., and Steglich, F. (2003). Low Temperature Electron Spin Resonance of the Kondo Ion in a Heavy Fermion Metal: YbRh₂Si₂. *Phys. Rev. Lett.* 91, 156401. doi:10.1103/physrevlett.91.156401
- Singh, S., Capan, C., Nicklas, M., Rams, M., Gladun, A., Lee, H., et al. (2007). Probing the Quantum Critical Behavior of CeCoIn₅ via Hall Effect Measurements. *Phys. Rev. Lett.* 98, 057001. doi:10.1103/PhysRevLett.98.057001
- Smidman, M., Stockert, O., Arndt, J., Pang, G. M., Jiao, L., Yuan, H. Q., et al. (2018). Interplay between Unconventional Superconductivity and Heavy-Fermion Quantum Criticality: CeCu₂Si₂ versus YbRh₂Si₂. *Philos. Mag.* 98, 2930–2963. doi:10.1080/14786435.2018.1511070
- Smith, M. F., and McKenzie, R. H. (2008). Apparent Violation of the Wiedemann-Franz Law Near a Magnetic Field Tuned Metal-Antiferromagnetic Quantum Critical Point. *Phys. Rev. Lett.* 101, 266403. doi:10.1103/physrevlett.101.266403
- Steglich, F., Aarts, J., Bredl, C. D., Lieke, W., Meschede, D., Franz, W., et al. (1979). Superconductivity in the Presence of Strong Pauli Paramagnetism: CeCu₂Si₂. *Phys. Rev. Lett.* 43, 1892–1896. doi:10.1103/physrevlett.43.1892
- Steglich, F., Pfau, H., Lausberg, S., Hamann, S., Sun, P., Stockert, U., et al. (2014). Evidence of a Kondo Destroying Quantum Critical Point in YbRh₂Si₂. *J. Phys. Soc. Jpn.* 83, 061001. doi:10.7566/jpsj.83.061001
- Stewart, G. R. (2001). Non-Fermi-Liquid Behavior in *d*- and *f*-Electron Metals. *Rev. Mod. Phys.* 73, 797–855. *ibid.* 78, 743–753 (2006). doi:10.1103/RevModPhys.73.797
- Stockert, O., Andreica, D., Amato, A., Jeevan, H. S., Geibel, C., and Steglich, F. (2006a). Magnetic Order and Superconductivity in Single-Crystalline CeCu₂Si₂. *Physica B: Condensed Matter* 374–375, 167–170. doi:10.1016/j.physb.2005.11.043
- Stockert, O., Koza, M. M., Ferstl, J., Murani, A. P., Geibel, C., and Steglich, F. (2006b). Crystalline Electric Field Excitations of the Non-Fermi-Liquid YbRh₂Si₂. *Physica B: Condensed Matter* 378–380, 157–158. doi:10.1016/j.physb.2006.01.059
- Sun, P., and Steglich, F. (2013). Nernst Effect: Evidence of Local Kondo Scattering in Heavy Fermions. *Phys. Rev. Lett.* 110, 216408. doi:10.1103/physrevlett.110.216408
- Tanatar, M. A., Paglione, J., Petrovic, C., and Taillefer, L. (2007). Anisotropic Violation of the Wiedemann-Franz Law at a Quantum Critical Point. *Science* 316, 1320–1322. doi:10.1126/science.1140762
- Taupin, M., Knebel, G., Matsuda, T. D., Lapertot, G., Machida, Y., Izawa, K., et al. (2015). Thermal Conductivity through the Quantum Critical Point in YbRh₂Si₂ at Very Low Temperature. *Phys. Rev. Lett.* 115, 046402. doi:10.1103/physrevlett.115.046402
- Taupin, M., and Paschen, S. (2022). Are Heavy Fermion Strange Metals Planckian? *arXiv:2201.02820*.
- Trovarelli, O., Geibel, C., Mederle, S., Langhammer, C., Grosche, F. M., Gegenwart, P., et al. (2000). YbRh₂Si₂: Pronounced Non-Fermi-Liquid Effects above a Low-Lying Magnetic Phase Transition. *Phys. Rev. Lett.* 85, 626–629. doi:10.1103/physrevlett.85.626
- von Löhneysen, H., Pietrus, T., Portisch, G., Schlager, H. G., Schröder, A., Sieck, M., et al. (1994). Non-Fermi-Liquid Behavior in a Heavy-Fermion Alloy at a Magnetic Instability. *Phys. Rev. Lett.* 72, 3262–3265. doi:10.1103/PhysRevLett.72.3262
- von Löhneysen, H., Rosch, A., Vojta, M., and Wölfle, P. (2007). Fermi-Liquid Instabilities at Magnetic Quantum Phase Transitions. *Rev. Mod. Phys.* 79, 1015–1075.
- Westerkamp, T. (2009). *Quantum Phase Transitions in the Heavy Fermion Systems Yb(Rh_{1-x}M_x)₂Si₂ and CePd_{1-x}Rh_x* (in German) (Germany: Technical University Dresden). Ph.D. thesis.
- Wirth, S., Ernst, S., Cardoso-Gil, R., Borrmann, H., Seiro, S., Krellner, C., et al. (2012). Structural Investigations on YbRh₂Si₂: from the Atomic to the Macroscopic Length Scale. *J. Phys. Condens. Matter* 24, 294203. doi:10.1088/0953-8984/24/29/294203
- Wirth, S., and Steglich, F. (2016). Exploring Heavy Fermions from Macroscopic to Microscopic Length Scales. *Nat. Rev. Mater.* 1, 16051. doi:10.1038/natrevmats.2016.51
- Wölfle, P., and Abrahams, E. (2011). Quasiparticles beyond the Fermi Liquid and Heavy Fermion Criticality. *Phys. Rev. B* 84, 041101. (R). doi:10.1103/physrevb.84.041101
- Zaum, S., Grube, K., Schäfer, R., Bauer, E. D., Thompson, J. D., and von Löhneysen, H. (2011). Towards the Identification of a Quantum Critical Line in the (*p*, *B*) Phase Diagram of CeCoIn₅ with Thermal-Expansion Measurements. *Phys. Rev. Lett.* 106, 087003. doi:10.1103/PhysRevLett.106.087003
- Zwicknagl, G. (2011). Field-Induced Suppression of the Heavy-Fermion State in YbRh₂Si₂. *J. Phys. Condens. Matter* 23, 094215. doi:10.1088/0953-8984/23/9/094215

Conflict of Interest: The authors declare that the research was conducted in the absence of any commercial or financial relationships that could be construed as a potential conflict of interest.

Publisher’s Note: All claims expressed in this article are solely those of the authors and do not necessarily represent those of their affiliated organizations, or those of the publisher, the editors and the reviewers. Any product that may be evaluated in this article, or claim that may be made by its manufacturer, is not guaranteed or endorsed by the publisher.

Copyright © 2022 Schuberth, Wirth and Steglich. This is an open-access article distributed under the terms of the Creative Commons Attribution License (CC BY). The use, distribution or reproduction in other forums is permitted, provided the original author(s) and the copyright owner(s) are credited and that the original publication in this journal is cited, in accordance with accepted academic practice. No use, distribution or reproduction is permitted which does not comply with these terms.